Article

A Facile, Label-free and Universal Biosensor Platform Based on Target-induced Graphene Oxide Constrained DNA Dissociation Coupling with Improved Strand Displacement Amplification

Zhijun Huang, Zewei Luo, Junman Chen, Ya Xu, and Yixiang Duan

ACS Sens., **Just Accepted Manuscript** • DOI: 10.1021/acssensors.8b00935 • Publication Date (Web): 18 Oct 2018

A Facile, Label-free and Universal Biosensor Platform Based on Target-induced Graphene Oxide Constrained DNA Dissociation Coupling with Improved Strand Displacement Amplification

Zhijun Huang, Zewei Luo, Junman Chen, Ya Xu, and Yixiang Duan*

Research Center of Analytical Instrumentation, Key Laboratory of Bio-Resource and Eco-Environment of Ministry of Education, College of Life Sciences, Sichuan University, Chengdu 610065, Sichuan, P.R. China

Abstract: In this work, we report a low-cost and easy operation biosensor platform capable of detection of various analytes with high sensitivity and good selectivity. By ingeniously assigning the specific aptamer into a primer-template integrated DNA template, and using monolayer graphene oxide as a reversible and nonspecific inhibitor, the simple biosensor platform is set up. Without target, DNA template is constrained by the graphene oxide sheet and result in low signal. In the presence of target, the constrained DNA template is released from the graphene oxide surface *via* target-induced aptamer conformational change, and further amplified through the improved strand displacement amplification reaction. Therefore, the target detection is simply converted to DNA detection, and a correlation between target concentration and fluorescence signal can be set up. As a result, dozens folds of signal enhancement, high sensitivity, good selectivity and potential practicability are achieved in target detection. More importantly, the proposed biosensor platform is versatile, meaning that it can greatly facilitate the detection of a variety of analytes. Due to the low-cost and easy availability of sensing materials, and the elimination of tedious detection operations, we believe that this simple and universal biosensor platform can find wide applications in biological assay and environment monitoring.

Keywords: Aptamer, Graphene oxide, Conformational change, Universal applicability, Improved strand displacement amplification

With the healthcare and environmental problems have received intense public attention in recent years, there is a growing need of sensitive analytical methods.[1-3] In analytical chemistry, many techniques are available for highly sensitive detection, and the methods such as digital PCR,[4-5] Raman microspectroscopy,[6] and mass spectra[7-8] can even achieve single molecule detection. However, expensive equipment, skilled operators as well as complex operation procedures are required in these analytical techniques, which greatly limited their wide applications in the work of daily testing. Therefore, the detection technique with the advantages of low-cost and easy operation also is highly desirable in daily testing. In biological assays and environmental monitoring, target detection by using biosensor is a simple and promising approach to achieve the above advantages, and many biosensors have been constructed to achieve sensitive detection of specific targets.[9-13] In addition to low-cost and easy operation, universal applicability is another important requirement for practical daily use. In the work of daily testing, especially in environment monitoring, it is often necessary to detect a variety of analytes. Therefore, much time can be saved if the detection of different targets can be implemented by using the same working principle and with little change. Through the application of excellent nanomaterials and ingenious biosensor designs, some reported biosensors are versatile,[14-18] which have greatly facilitated the daily testing.

2D nanomaterial graphene oxide (GO) has recently attracted great attention for biosensor applications due to its outstanding properties.[18-21] It is well known that the single-stranded aptamers can be anchored onto the GO sheet *via* π-π stacking,[22-25] and that the constrained DNA aptamers can be released when the specific target-aptamer interaction occurs.[18, 26-27] Based on the simple and specific interactions, many GO based biosensors have been reported for the detection of various targets.[15, 19, 22, 28] Among the GO based versatile biosensors, an effective signal amplification process always provides high sensitivity. The strategies of nuclease-assistant digestion of DNA aptamers[2, 28] as well as rolling circle amplification (RCA)[15, 21] are most frequently used. Unfortunately, there are some drawbacks among the above-mentioned amplification strategies. For the strategy of nuclease-assistant aptamer digestion, the labeled DNA aptamers are always needed, which make the constructed biosensors expensive. Moreover, the digestion strategy might encounter a steric hindrance in protein detection.[15, 29] These drawbacks have

limited utilization of the nuclease-assistant digestion strategy. When the RCA strategy is applied, the extra operations like DNA ligation, DNA purification and the primer-template ratio adjustment are always required,[15, 30-31] which could be difficult for some unskilled operators. Therefore, building versatile biosensor platform through different strategy to achieve the advantages of low-cost and easy operation is advisable and meaningful.

Besides the above-mentioned signal amplification strategies, the strand displacement amplification (SDA) reaction is also used to construct GO based biosensors.[32] However, the tedious operation of DNA primer-template ratio adjustment is still necessary in the typical SDA strategy, which may increase the complexity of the sensor system and reduce the sensitivity. In order to simplify the biosensor platform and the testing operation, the improved strand displacement amplification (ISDA) reaction was used to achieve cascade signal amplification in this study. In the ISDA reaction, a primer-template integrated DNA template was used, which can omit the step of primer-template ratio adjustment, while ensuring very efficient DNA amplification. Through assigning the aptamer sequence in a specific domain of the DNA template, the DNA template can dissociate from the GO surface in the presence of correct target, and the released DNA template can further trigger cascade signal amplification. As a result, the produced fluorescence signal was greatly enhanced by the ISDA reaction, and a linear relationship between the target concentration and generated signal can be finally set up. Based on the simple mechanism, three simple biosensors were constructed to detect thrombin, Pb^{2+} and ssDNA, with high sensitivity, good selectivity, and their potential for practical use was evaluated as well. According to the good performance of constructed biosensors, it is reasonable to believe that this simple and versatile biosensor platform is suitable for detecting biological and environmental samples in the daily routine analysis.

Results and Discussion

Working Principle of the GO Based ISDA Biosensor Platform.

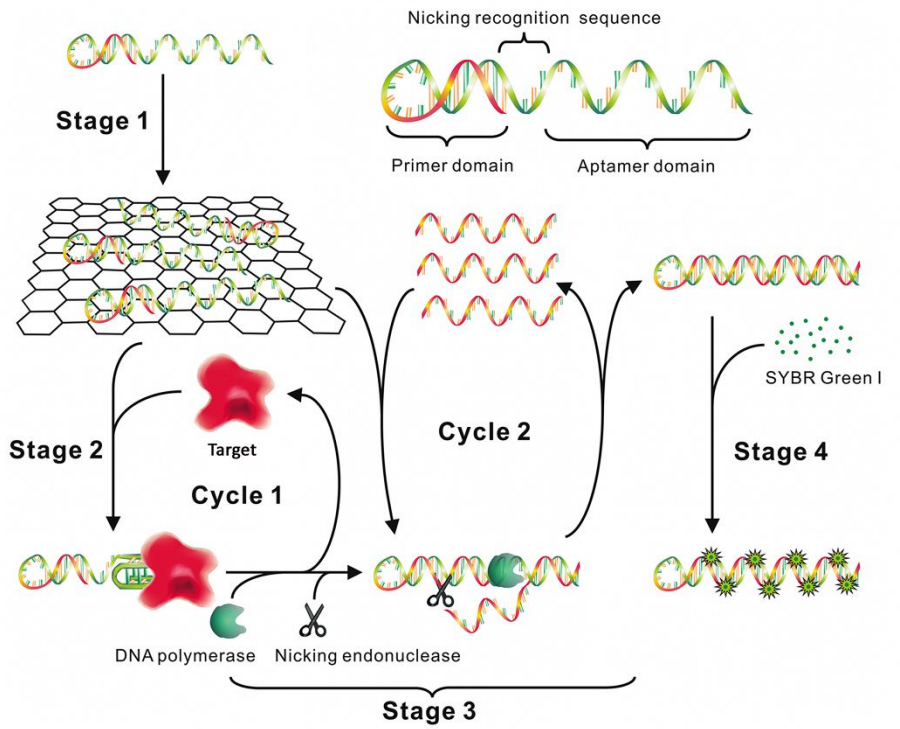

Scheme 1. Scheme of the GO based ISDA biosensor platform.

The working principle of the GO based ISDA biosensor platform is schematically illustrated in **Scheme 1**. In this study, an integrated primer-template DNA strand (denoted as DNA template) was used to construct the improved strand displacement amplification (ISDA) reaction. As shown in **Scheme 1**, the DNA template can be simply divided into three domains. A primer domain folding into a hairpin structure is at the 3'-end of the template, which ensures an efficient initiation of the ISDA reaction. The recognition sequence of the nicking endonuclease is in the middle of the template, which is important for the formation of the second signal amplification cycle (the cDNA cycle) in our study. The single-stranded aptamer domain is at the 5'-end of the template and serves as a highly specific recognition element. With its aptamer domain in a single-stranded form, the DNA template is anticipated to anchor onto the GO sheet through π-π interactions in the absence of target (stage 1 in **Scheme 1**). By contrary, in the presence of target, the target-aptamer interaction can induce a conformational change in the aptamer domain, which results in the dissociation of the DNA-target complex (stage 2 in **Scheme 1**). In the first two stages, the simple biosensor can be considered to be a simple GO based versatile biosensor without the process of signal amplification.[22] However, since one target molecule usually releases only one

aptamer, without an effective signal amplification process, this kind of GO based biosensor provides limited sensitivity.[22, 28]

To achieve higher sensitivity, the ISDA reaction was applied for signal amplification in this study. It was reported that DNA can bind to the surface of GO and effectively prevent nuclease digestion.[33-36] Some theories, including changes in DNA conformation,[37] changes in local ionic concentration,[33, 38] and the most popular theory of steric hindrance effect,[33-36, 39-40] were used to explain this phenomenon. Although the mechanism was still elusive, this useful property was utilized in this biosensor platform. The enzymatic DNA amplification reaction was also inhibited when the DNA template was bound to the GO surface.[15, 21, 33] However, since this inhibition is not caused by enzyme inactivation and is reversible, the ISDA reaction can be restarted once the DNA template is released from the GO surface. Therefore, in the absence of target, the DNA template was still constrained on the GO sheet and was not amplified. In contrast, when the constrained DNA template was released by target, the ISDA reaction was restarted, and two cycles contributing to DNA amplification can take place (stage 3 in **Scheme 1**). In this biosensor platform, the target cycle (cycle 1 in **Scheme 1**) is realized by the strand displacement activity of the DNA polymerase,[41-43] and a huge amount of cDNA is generated by the cooperative action of DNA polymerase and nicking endonuclease.[44] According to the simple rule of Waston-Crick base pairing, as a product of DNA extension reaction, the generated cDNA is completely complementary to the aptamer domain of the DNA template. Therefore, the generated cDNA can induce a DNA conformational change and hybridize with the DNA template to form a complete dsDNA structure. Owing to the fact that dsDNA binds GO with low affinity, the form dsDNA can release from GO surface.[23] Hence, once the cDNA is generated, the cDNA cycle (cycle 2 in **Scheme 1**) is also realized. As a result, in the presence of the correct target, the constrained DNA template is released and extended to be a complete dsDNA, and the target detection is simply converted to DNA detection. By further staining the produced dsDNA with fluorescent dye, a correlation between the generated fluorescence signal and the target concentration can be finally set up.

More importantly, because the ssDNA can strongly anchor onto GO surface *via* π-π stacking with less sequence specificity,[22-23] the detection of different targets can be achieved by simply varying the

aptamer domain in the DNA template. In this study, two additional biosensors were built to verify the versatility of the biosensor platform, which are shown below.

Characterizations of the Monolayer GO. As a DNA carrier and a nonspecific inhibitor, the quality of GO was found to be crucial for the performance of the constructed biosensors. The GO applied in this study was synthesized according to the modified Hummers method[45] (see Supplementary Information for more details), and the resultant GO was further characterized by atomic force microscopy (AFM), transmission electron microscopy (TEM), Raman spectroscopy, flourier transform infrared (FTIR) spectroscopy, and Tyndall effect.

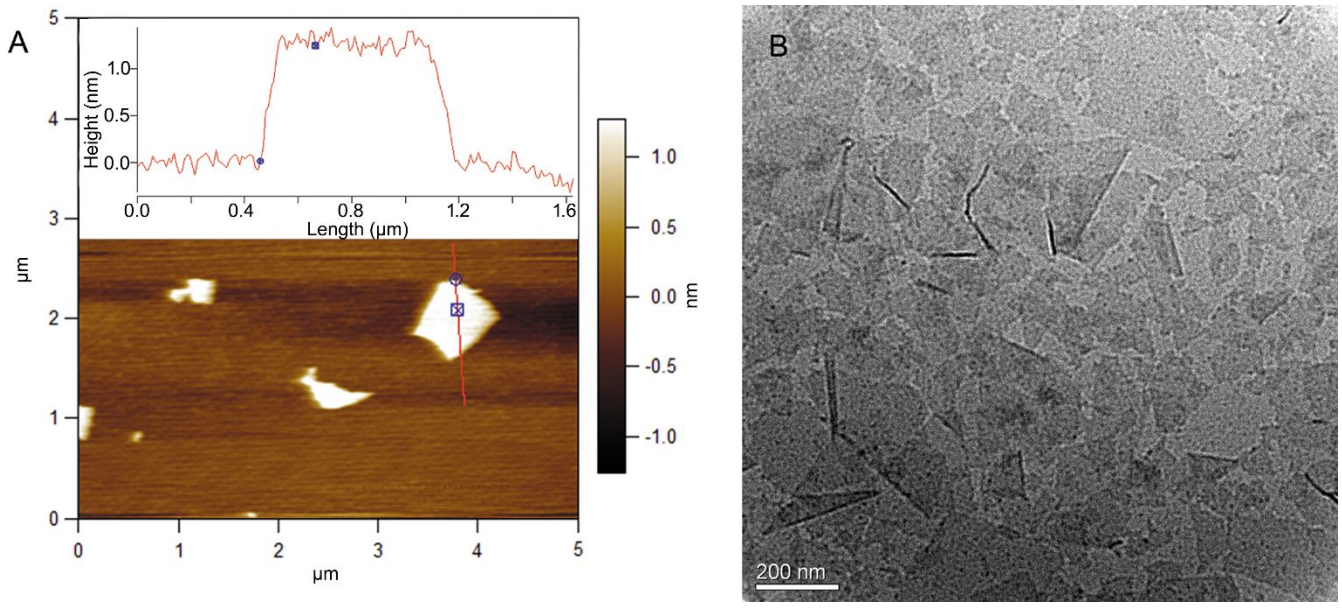

Figure 1. Characterizations of the monolayer GO sample. (A) AFM image of the synthesized GO deposited on freshly cleaved mica substrate, the inset showed the height profile of the GO sheet. (B) TEM image of the synthesized GO.

As shown by the AFM image and the height profile in **Figure 1A**, the generated GO showed an average thickness of about 1.2 nm, indicating a single layered GO was synthesized.[22-23, 45-46] In the TEM image (**Figure 1B**), the generated GO showed a relatively uniform size, which is beneficial for constructing homogeneous biosensors. Besides, owing to the richness of oxygen-containing functional groups in the GO sheet, the generated GO showed good solubility and dispensability in water,[15, 45] and the stable colloidal nature of the monolayer GO was reflected by the Tyndall effect (**Figure S1A** inset). Moreover,

some characteristic spectral peaks of the typical GO[45-47] were also identified by the Raman and FTIR spectroscopy respectively (**Figure S1A and S1B)**.

Accordingly, we can deduce that GO monolayers with good solubility and dispensability were successfully synthesized, and they were diluted and applied to construct the GO based ISDA biosensor platform in this study.

Verification the Feasibility of the GO Based ISDA Biosensor Platform. It is well known that the fluorescence resonance energy transfer (FRET) can occur between the dye-labeled DNA and the monolayer GO sheet.[22, 48] Thanks to the excellent fluorescence quenching ability of GO, the process of DNA adsorption and desorption can be reflected by the fluctuation of the fluorescence signal when a dye-labeled DNA template is used.

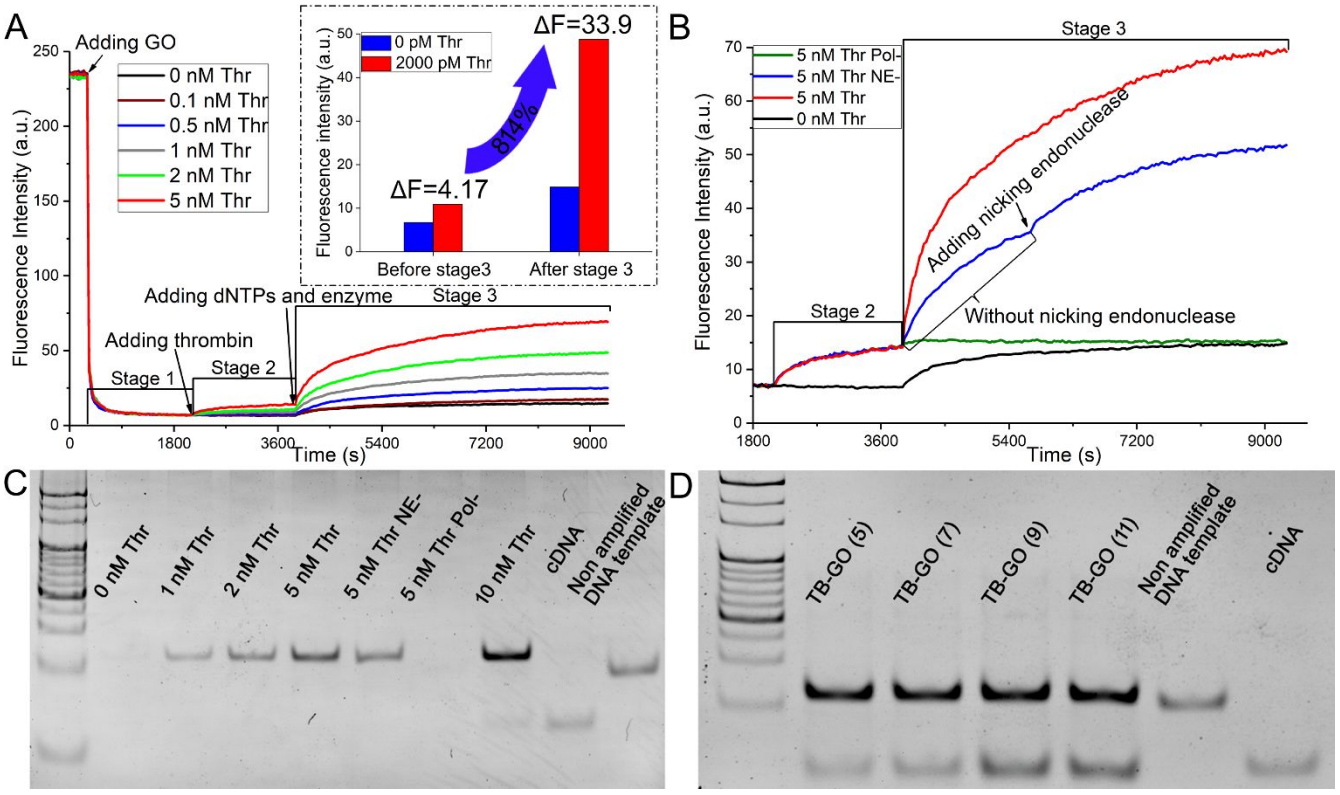

Figure 2. Verification the feasibility of the GO based ISDA biosensor platform. (A) The time-dependent fluorescence kinetics of the thrombin biosensor, in which the FAM-labeled DNA template was used. The inset showed a great fluorescence enhancement was achieved after the stage 3. (B) The kinetics curve with (curve 5 nM Thr) or without (curve 5 nM Thr Pol-) an effective amplification stage. And the kinetics curve when the nicking endonuclease was added delayed (curve 5nM Thr NE-). (C) PAGE results of the DNA products generated by the fluorescence kinetics. (D)

Optimizing the primer length of DNA template. 50 nM of different DNA templates were amplified at 37°C for 30 min in the absence of GO and thrombin, the ISDA reaction was performed in 1× binding buffer A (100 mM NaCl, 5 mM $MgCl_2$, 20mM Tris-HCl, pH 7.4).

As shown in **Figure 2A**, three distinct stages were observed, which corresponding to the three stages in the **Scheme 1**. Moreover, as shown by the kinetics curve, the generated fluorescence signal was very weak in the first two stages. This is because without a process of signal amplification, only limited amount of FAM-labeled DNA template can be released by the thrombin directly.[22] However, upon the addition of deoxy-ribonucleoside triphosphate (dNTPs), DNA polymerase and nicking endonuclease, a drastic increase of fluorescence signal was observed (stage 3 in **Figure 2A and 2B**). In this GO based ISDA biosensor platform, the rise of fluorescence may be caused by a nonspecific competition between the newly added reagents and the constrained DNA template, or likely by the occurrence of the ISDA reaction. To test the above hypothesis, a simple control trial was setup. As shown in **Figure 2B**, it was found that very low fluorescence signal was produced without the occurrence of effective ISDA reaction (curve 5 nM Thr Pol-, in which 5 nM of thrombin was tested but the added DNA polymerase was heated-inactivated). With the gathered information, it can be deduced that the ISDA reaction can be restarted in the presence of target, and the drastic fluorescence signal was mainly caused by the process of ISDA reaction, while the fluorescence fluctuation induced by the newly added reagents was negligible. To verify that the added nicking endonuclease was helpful for signal amplification, another simple control trial was setup. As a result, when the nicking endonuclease was not added, the produced fluorescence signal was obviously weaker. But once upon the nicking endonuclease was added into the system, a significant change of the rate fluorescence growth was observed (the curve 5 nM Thr NE-, in which the addition of nicking endonuclease was delayed for 30 min). This is because the cDNA cannot be produced without the action of nicking endonuclease, and the target cycle (cycle 1 in **Scheme 1**) results in a relative slow rise of the fluorescence signal. However, once the cDNA was produced by the combined action of DNA polymerase and nicking endonuclease, the cDNA cycle (cycle 2 in **Scheme 1**) was realized, leading to an increased in the rate of fluorescence growth. In addition, it was found that the PAGE results were

consistent with the kinetics curve. A DNA band with the size of complete dsDNA was found in the lanes with active DNA polymerase (**Figure 2C**, the lane 1nM Thr, 2nM Thr and 5 nM Thr), Whereas a DNA band with a size close to the DNA template was almost invisible in the control lane (**Figure 2C**, the lane 5 nM Thr Pol-).

Considering the above results, it can be concluded that once the constrained DNA template is released through target-induced, it can be effectively amplified and trigger cascade signal amplification cycles. Since the DNA template released from GO surface is caused by target, it is believed that the target concentration is correlated with generated signal.

Optimization of Experimental Conditions.

Optimization of the DNA template. In the proposed GO based ISDA versatile biosensor platform, an effective ISDA reaction can improve the sensitivity of the biosensor platform. Since the DNA loop is in the ssDNA form and ssDNA binds GO with high affinity,[22-25] it is believed that too long a loop will weaken the release of DNA template responding to target-aptamer interactions. The length of DNA loop was optimized by using the online software NUPACK (http://www.nupack.org/), and the 5 nt DNA loop was used in this study according to the simulation results (**Figure S2).** Besides, the DNA templates with different primer length (the length of the complementary stem, the corresponding sequence is listed in **Table S1**) were compared through the DNA amplification results. As a result, it was found that DNA templates with shorter primer domain were more difficult to extend into a complete dsDNA and less cDNA were generated by comparing to those produced by DNA templates with longer primer (**Figure 2D**). This is mainly because a certain length of complementary base pairs is necessary for the formation of a stable hairpin structure, and the ISDA reaction occurs only when the correct conformation is formed. Finally, the DNA template with a primer length of 9 nt was used for biosensor construction. In this work, the FAM-labeled DNA template was utilized to monitor the time-dependent fluorescence kinetics (the molecular structure of fluorescence dye is shown in **Figure S3**). Moreover, as mentioned above, the detection of different targets can be achieved by simply replacing the aptamer domain, which can save much time in the process of DNA sequence optimization. In this study, two additional biosensors were

built to detect Pb^{2+} and ssDNA respectively, and all the DNA sequences were listed in the **Table S1** in the supplementary material.

Optimization of the used GO concentration. The GO-DNA interaction is a dynamic equilibrium process. Accordingly, the amount of GO used for adsorbing DNA template could affect the performance of the constructed biosensors, therefore, the GO concentration needs to be adjusted. For the thrombin biosensor construction, the time-dependent DNA adsorption kinetics was set up to determine the appropriate GO concentration. As shown in **Figure S4A**, the adsorption process was rapid, and finally a GO concentration of 9 μg/mL was used for the thrombin biosensor construction. For the other two simple biosensors, the optimum concentrations of GO were adjusted according to the signal to background ratio (**Figure S4B and S4C)**, and the GO concentration of 10 μg/mL and 11 μg/mL were used to construct the Pb^{2+} biosensor and ssDNA biosensor, respectively.

Optimization of the used amount of enzyme. Besides the structure of DNA template and the used GO concentration, the amount of enzyme used for DNA amplification was also investigated in this study. As shown in **Figure S5A**, both the background and signal were increased when more amount of enzyme was used. However, it was found that the signal to background ratio reached the maximum when 2.5 U of DNA polymerase and 5 U of nicking endonuclease were used, therefore this amount of enzyme was used for all the detection.

Comparison of the two signal generation approaches. In this study, two simple methods can be used for fluorescence signal generation. One is by using a fluorescent-labeled DNA template (high-cost, not easy to store, can monitor the reaction kinetics). The other is by staining the generated dsDNA with a fluorescent dye (low-cost, easy to store, and more sensitive). As shown in **Figure S5B**, the fluorescence signal produced by both methods showed good linear relationship with the DNA concentration, and it was also found that the fluorescence signal generated by the post-staining method was much stronger. Therefore, the post-staining approach was employed for signal generation in this study (see

Supplementary Information for more details).

Sensitivity of the Biosensor Platform. In this study, three biosensors were built to detect thrombin, Pb^{2+} and ssDNA respectively, and all these biosensors have achieved high sensitivity. As shown in **Figure 3A** inset, through the action of ISDA reaction, the fluorescence signal was greatly enhanced (36 folds of enhancement in fluorescence difference was achieved when 2 nM of thrombin was detected). Further, as shown in **Figure 3B**, by using the simple biosensor platform for thrombin detection, in the range of 50 pM to 2000 pM, the intensity of the generated fluorescence showed a good linear correlation with the concentration of thrombin, and a limit of detection (LOD, defined as 3σ/S, σ refers to the standard deviation of the blank samples, and S refers to the slope of the fitting standard curve) of 22.8 pM was achieved.

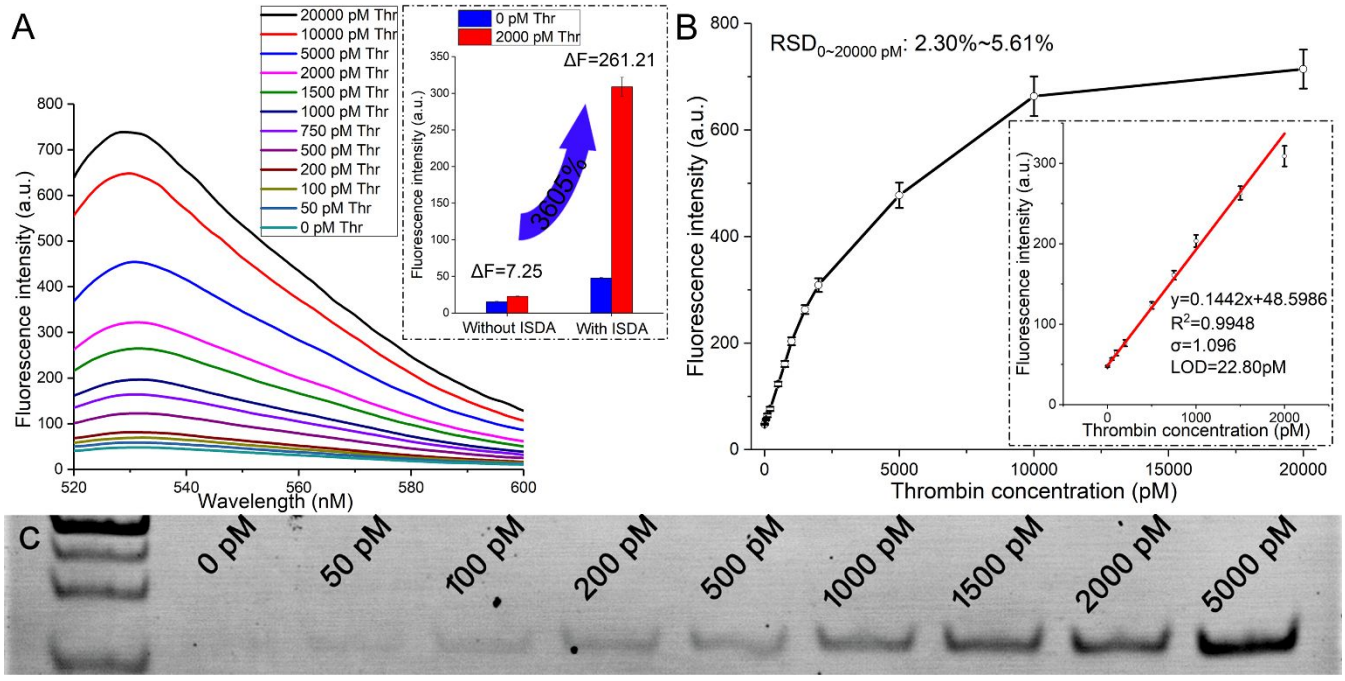

Figure 3. Performance of the constructed thrombin biosensor. (A) The produced fluorescence spectra when different concentrations of thrombin were tested. The inset showed that the fluorescence signal was greatly enhanced by the ISDA reaction. (B) Linear relationship between fluorescence intensity and thrombin concentration. (C) PAGE results of the produced dsDNA. (All the data were of five independent repeats).

As shown in **Figure S6**, for the detection of Pb^{2+}, by simply changing the DNA template and adjust the

GO concentration, in the range of 100 pM to 1500 pM, a good linear correlation between the fluorescence intensity and the Pb^{2+} concentration was achieved, and the LOD of 86.2 pM was obtained (20 folds of enhancement in fluorescence difference was achieved when 1.5 nM of Pb^{2+} was detected). In our study, the LOD of 86.2 pM is much lower than the maximum contamination level of 72 nM for Pb^{2+} in drinking water as defined by the U.S. Environmental Protection Agency.[49]

In addition, by changing the aptamer into the complementary sequence of target DNA, the simple biosensor platform can be used for ssDNA detection. In this study, a Porcine circovirus 2 (PCV2) DNA was tested. As shown in **Figure S7**, in the range of 10 pM to 500 pM, the generated fluorescence signal showed a good linear correlation with the PCV2 DNA concentration, and a LOD of 5.2 pM was obtained (73 folds of enhancement influorescence difference was achieved when 500 pM of PCV2 DNA was detected).

Compared with the reported biosensors, the simple biosensor platform showed good sensitivity (**Table S2**). More importantly, by using the monolayer GO as a nonspecific inhibitor and using the highly specific aptamers as target recognition element, the proposed biosensor platform is versatile, which can be used to detect different analytes by simply replacing the DNA template. We believe that the universal applicability of the platform is an important and useful advantage to simplify the work of daily testing.

Selectivity of the Biosensor Platform. In addition to high sensitivity and universal applicability, good selectivity is another important property a biosensor should have. Therefore, the selectivity of the biosensor platform was also evaluated in this study. For the simple biosensor platform, its ability of distinguishing correct targets from their structural analogues is mainly attributed to the high affinity of DNA aptamers, and is also affected by cognate targets that compete with constrained DNA for the binding sites on GO surface.

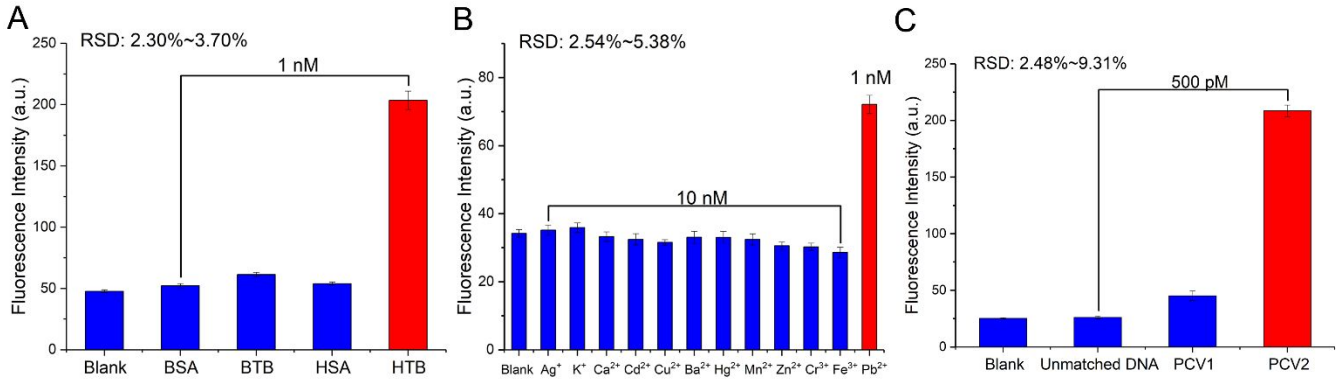

Figure 4. The selectivity of the constructed biosensors. (A) Thrombin biosensor can discriminate human thrombin from bovine serum albumin, bovine thrombin and human serum albumin. (B) Pb^{2+} biosensor can discriminate Pb^{2+} from other cations. (C) The ssDNA biosensor can discriminate target DNA from unmatched DNA or single-base mismatched DNA.

As shown in **Figure 4**, target analogues were tested by the three built biosensors respectively. Through comparing the fluorescence signal generated by the correct targets and their analogues, it was found that the thrombin biosensor can discriminate human thrombin (HTB) from bovine serum albumin (BSA), bovine thrombin (BTB) and human serum albumin (HSA) (**Figure 4A**). The Pb^{2+} biosensor can discriminate Pb^{2+} from some other kinds of cations (**Figure 4B**). And the ssDNA biosensor can discriminate target DNA from single-base mismatched DNA or the unmatched DNA (**Figure 4C**). Considering the above results, it can be concluded that the simple biosensor platform has good selectivity.

The Performance of Biosensor Platform in Complex Matrices. After having demonstrated the high sensitivity, universal applicability and good selectivity of the simple biosensor platform, the performance in complex matrices was further investigated to access the usefulness for practical applications. For the constructed thrombin biosensor, detection was carried out in diluted calf serum. As shown in **Figure 5A**, the background signal gradually raised with the increase of calf serum concentration. This is mainly because the abundant protein in the calf serum can dissociate the constrained DNA template through nonspecific competition, and the nonspecific initiation of ISDA results in the increase of the background signal. In addition, some unknown components in the serum may also cause significant background signal or inhibit the DNA amplification reaction, and these combined effects eventually lead to a

decrease in the detection sensitivity. However, although the background signal and the LOD became larger with the increase of serum concentration, the intensity of generated fluorescence signal and the thrombin concentration still maintained a good linear relationship (**Figure 5B**). Therefore, the thrombin detection can be carried out in diluted serum, and a good linear relationship can be maintained between generated signal and thrombin concentration.[15, 50-51] For the constructed ssDNA biosensor, DNA detection was also investigated in diluted calf serum. The results shown in **Figure S8** confirmed that ssDNA detection can also be carried out in diluted serum.

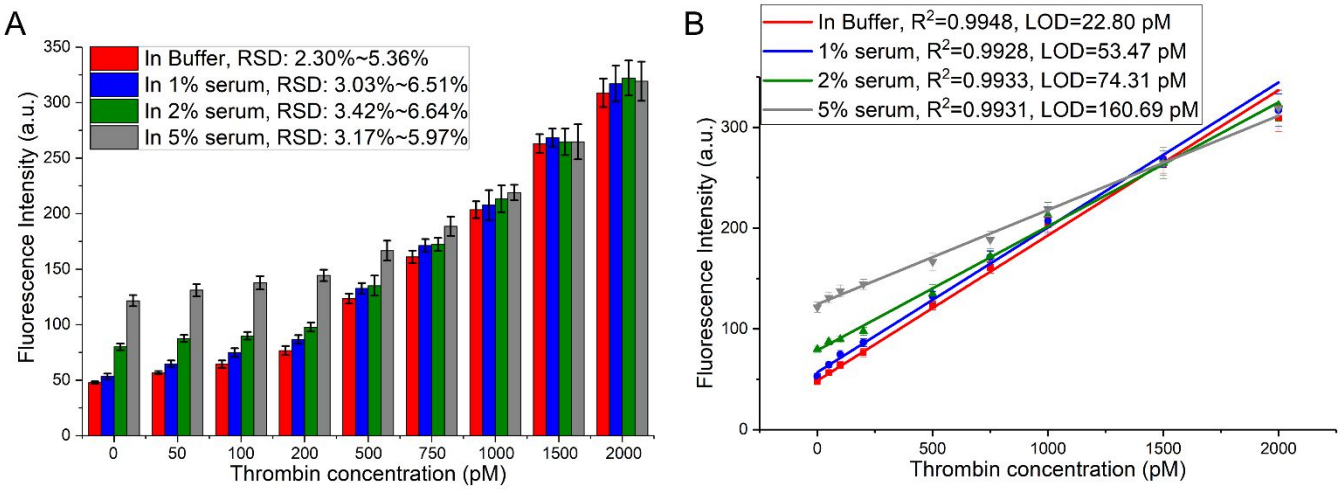

Figure 5. (A) The performance of thrombin biosensor in diluted serum. (B) The linear relationship between the generated fluorescence signal and thrombin concentration when target detection was carried out in diluted serum. (All the data were of five independent repeats).

For the Pb^{2+} biosensor, its performance was tested with Pb^{2+} stock solution spiked in pond water that was diluted by ultrapure water at the ratios of 1:4 and 1:1, and the recoveries were 94.0% and 105.8%, respectively (**Table 1**). All these results showed that the target detection can be carried out in complex matrices, and it is reasonable to anticipate that the simple biosensor platform can find wide applications in real sample analysis.

Table 1. Analysis of Pb^{2+} in diluted pond water[a] (n=5)

Dilution ratio[b]	Pb^{2+} in diluted pond water (pM)	Added Pb^{2+} (pM)	Detected Pb^{2+} (pM)	RSD (%)	Recovery (%)

1:4	342.4	1000	1400.4	5.1	105.8
1:1	821.1	500	1282.4	5.9	94.0

[a] The mean concentrations were calculated by the linear curve of the constructed Pb^{2+} biosensor. [b] The ratio of pond water and ultrapure water.

Conclusions

In summary, we have developed a simple and novel biosensor platform that can detect both small-molecules and macro-molecules with high sensitivity and good selectivity. The simple biosensor platform was constructed based on the mechanism of target-induced graphene oxide-constrained DNA template dissociation coupling with improved strand displacement amplification, which has achieved many advantages. Firstly, by using an isothermal DNA amplification strategy and the post-staining method rather than a DNA aptamer digestion strategy, the biosensor platform was label-free and cost-effective. Secondly, by using the highly integrated DNA template, some tedious operations were omitted, making the biosensor platform easy to operate and suitable for daily testing. Thirdly, by using the highly specific DNA aptamers as target recognition elements and using the monolayer GO as a nonspecific blocker, both good selectivity and universal applicability were achieved. In addition, it was found that the simple biosensor platform also achieved good performance in complex matrices. Given the advantages of the proposed biosensor platform to facilitate daily testing, we believe that the universal, cost-effective and convenient biosensor platform can be widely applied in the detection of biological and environmental samples.

Methods

Oligonucleotides and Reagents. All the DNA oligonucleotides (**Table S1**) were synthesized by Shanghai Sangon Biotechnological Co., Ltd. (Shanghai, China), dissolved and directly used without further purification. Klenow Fragment, exo- (5 U/μL) DNA polymerase was purchased from Thermo Scientific (Shanghai, China), and the nicking endonuclease Nb.BbvCI was purchased from New England Biolabs

(Ipswich, Massachusetts). The dNTPs mixture (2.5mM each) was purchased from TaKaRa Biotechnology Co., Ltd. (Dalian, China), and the SYBR Green I (10,000 × concentrated stock in H_2O) was purchased from Bio Teke Corporation (Beijing, China). Human thrombin, human serum albumin and bovine serum albumin were purchased from Sigma-Aldrich (Oakville, Canada). Bovine thrombin was purchased from Bersee Biotechnology Co., Ltd (Beijing, China), and the calf serum was purchased from Aoke Biotechnology Co., Ltd (Chengdu, China). Other chemical reagents were of A.R. Grade and ultrapure water (resistivity = 18.25 MΩ·cm) was used throughout the work.

Apparatus. The fluorescence measurements were performed by using a LS55 fluorescence spectrophotometer (PerkinElmer, USA) with an excitation wavelength (λex) of 497 nm. The slits for excitation and emission were set at 10 nm and 20 nm for all the experiments, except for **Figure S5B** (excitation and emission slits were set at 12.5 nm and 20 nm). Polyacrylamide gel electrophoresis analysis (PAGE) gel imaging was operated by an Azure c300 Biosystem (Azure Biosystems, USA). Atomic force microscopy (AFM) measurements were implemented by MFP-3D BIO. (Oxford Instruments, Abingdon, UK). Transmission electron microscopy (TEM) measurements were carried out using a FEI Tecnai G2 F20 S-T WIN instrument (FEI, USA). Raman spectra measurements were recorded by a LabRAM HR Raman spectrometer (HORIBA Scientific, Paris, France) with a He-Ne laser excitation of 532 nm. And flourier transform infrared (FTIR) spectroscopy were recorded by a Spectrum 100 (PerkinElmer, USA).

Target Detection and Kinetics Curve Construction. For a typical thrombin detection experiment, 100 μL of 10× binding buffer A (1000 mM NaCl, 50 mM $MgCl_2$, 200 mM Tris-HCl, pH 7.4), 50 μL of 1 μM DNA template, and 700 μL of water were mixed, kept at 95 ℃ for 5 min, and annealed to 25 ℃ with a rate of 0.1 ℃/s. Then, 100 μL of 90 μg/mL GO was added into the above mixture and incubated at 37 ℃ for 30 min. Subsequently, 95 μL of the above stock solution was transferred into a 200 μL PCR tube, and 2 μL of thrombin stock solution (0-1 μM) were added into. Followed by a further incubation at 37 ℃ for 30 min, 0.5 μL of exo- klenow DNA polymerase (5 U/μL), 0.5 μL of Nb.BbvCI (10 U/μL) and 2 μL of dNTPs (2.5 mM each) were introduced into the above mixture (reach a total volume of 100 μL). The reaction mixture was incubated at 37 ℃ for another 1.5 h, and 90 μL of reaction mixture was incubated with 10 μL of 20× SG (10,000 × concentrated stock SG was diluted by 1× binding buffer to reach a 20× working

concentration) at 37 ℃ for 5 min before fluorescence testing. The fluorescence spectrum at λem = 530 nm was recorded. (See the Supplementary Information for the procedure of Pb^{2+} and ssNDA detection). The detection procedure of time-dependent fluorescence kinetics was similar to the typical thrombin detection, except that the FAM-labeled DNA template was used and without further SG staining and a time-dependent fluorescence spectrum at λex/λem = 497/527 nm was recorded.

Polyacrylamide Gel Electrophoresis Analysis. The PAGE analysis was took place in 12% PAGE gel, in which 10 μL sample was run at 120 V for 45 min, followed by staining and PAGE gel imaging.

ASSOCIATED CONTENT

Supporting Information

The Supporting Information is available free of charge on the ACS Publications website

Additional tables and figures showing the applied DNA oligonucleotides, material characterization results, and other experimental results.

AUTHOR INFORMATION

Corresponding Author

* E-mail: yduan@scu.edu.cn.

ORCID

Yixiang Duan: 0000-0002-2333-4586

Author Contributions

The experiments were designed and performed by Zhijun Huang. Data analysis was performed by Zhijun Huang, Zewei Luo and Ya Xu. Manuscript was written by Zhijun Huang, modified by Junman Chen and Yixiang Duan.

Notes

The authors declare no competing financial interest.

Acknowledgments

This research was gratefully supported by the National Natural Science Foundation of China (No.

21874095).

References

1. Valentini, P.; Galimberti, A.; Mezzasalma, V.; Mattia, F. D.; Casiraghi, M.; Labra, M.; Pompa, P. P., DNA Barcoding Meets Nanotechnology: Development of a Universal Colorimetric Test for Food Authentication. *Angew. Chem. Int. Ed.* **2017,** *56* (28), 8094-8098.

2. Wei, Y.; Li, B. M.; Wang, X.; Duan, Y. X., Magnified fluorescence detection of silver(I) ion in aqueous solutions by using nano-graphite-DNA hybrid and DNase I. *Biosens. Bioelectron.* **2014,** *58*, 276-281.

3. Wu, Z. K.; Fan, H. H.; Satyavolu, N. S. R.; Wang, W. J.; Lake, R.; Jiang, J. H.; Lu, Y., Imaging Endogenous Metal Ions in Living Cells Using a DNAzyme-Catalytic Hairpin Assembly Probe. *Angew. Chem. Int. Ed.* **2017,** *56* (30), 8721-8725.

4. Ludlow, A. T.; Robin, J. D.; Sayed, M.; Litterst, C. M.; Shelton, D. N.; Shay, J. W.; Wright, W. E., Quantitative telomerase enzyme activity determination using droplet digital PCR with single cell resolution. *Nucleic Acids Res.* **2014,** *42* (13), e104.

5. Tian, H.; Sun, Y. Y.; Liu, C. H.; Duan, X. R.; Tang, W.; Li, Z. P., Precise Quantitation of MicroRNA in a Single Cell with Droplet Digital PCR Based on Ligation Reaction. *Anal. Chem.* **2016,** *88* (23), 11384-11389.

6. Wagner, M., Single-cell ecophysiology of microbes as revealed by Raman microspectroscopy or secondary ion mass spectrometry imaging. *Annu Rev Microbiol.* **2009,** *63*, 411-429.

7. Schober, Y.; Guenther, S.; Spengler, B.; Rompp, A., Single cell matrix-assisted laser desorption/ionization mass spectrometry imaging. *Anal. Chem.* **2012,** *84* (15), 6293-6297.

8. Svatos, A., Single-cell metabolomics comes of age: new developments in mass spectrometry profiling and imaging. *Anal. Chem.* **2011,** *83* (13), 5037-5044.

9. Tang, J. L.; He, X. X.; Lei, Y. L.; Shi, H.; Guo, Q. P.; Liu, J. B.; He, D. G.; Yan, L. A.; Wang, K. M., Temperature-responsive split aptamers coupled with polymerase chain reaction for label-free and sensitive detection of cancer cells. *Chem. Commun.* **2017,** *53* (87), 11889-11892.

10. Wang, S.; Zhang, L. Q.; Wan, S.; Cansiz, S.; Cui, C.; Liu, Y.; Cai, R.; Hong, C. Y.; Teng, I. T.; Shi, M. L.; Wu, Y.; Dong, Y. Y.; Tan, W. H., Aptasensor with Expanded Nucleotide Using DNA Nanotetrahedra for Electrochemical Detection of Cancerous Exosomes. *Acs Nano* **2017,** *11* (4), 3943-3949.

11. You, M. X.; Zhu, G. Z.; Chen, T.; Donovan, M. J.; Tan, W. H., Programmable and multiparameter DNA-based logic platform for cancer recognition and targeted therapy. *J. Am. Chem. Soc.* **2015,** *137* (2), 667-674.

12. Hao, N.; Hua, R.; Chen, S. B.; Zhang, Y.; Zhou, Z.; Qian, J.; Liu, Q.; Wang, K., Multiple signal-amplification via Ag and TiO2 decorated 3D nitrogen doped graphene hydrogel for fabricating sensitive label-free photoelectrochemical thrombin aptasensor. *Biosens. Bioelectron.* **2018,** *101*, 14-20.

13. Zhou, Z.; Hao, N.; Zhang, Y.; Hua, R.; Qian, J.; Liu, Q.; Li, H. N.; Zhu, W. H.; Wang, K., A novel universal colorimetric sensor for simultaneous dual target detection through DNA-directed self-assembly of graphene oxide and magnetic separation. *Chem. Commun.* **2017,** *53* (52), 7096-7099.

14. Li, T.; Liu, L.; Li, Y. R.; Xie, J. N.; Wu, H. C., A universal strategy for aptamer-based nanopore sensing through host-guest interactions inside alpha-hemolysin. *Angew. Chem. Int. Ed.* **2015,** *54* (26), 7568-7571.

15. Liu, M.; Song, J. P.; Shuang, S. M.; Dong, C.; Brennan, J. D.; Li, Y. F., A Graphene-Based Biosensing Platform Based on the Release of DNA Probes and Rolling Circle Amplification. *Acs Nano* **2014,** *8* (6), 5564-5573.
16. Wang, K.; Ren, J. T.; Fan, D. Q.; Liu, Y. Q.; Wang, E. K., Integration of graphene oxide and DNA as a universal platform for multiple arithmetic logic units. *Chem. Commun.* **2014,** *50* (92), 14390-14393.
17. Yan, L. A.; Shi, H.; He, X. X.; Wang, K. M.; Tang, J. L.; Chen, M.; Ye, X. S.; Xu, F. Z.; Lei, Y. L., A versatile activatable fluorescence probing platform for cancer cells in vitro and in vivo based on self-assembled aptamer/carbon nanotube ensembles. *Anal. Chem.* **2014,** *86* (18), 9271-9277.
18. Zhang, S. Q.; Wang, K.; Li, K. B.; Chen, F. Z.; Shi, W.; Jia, W. P.; Zhang, J.; Han, D. M., A label-free and universal platform for the construction of an odd/even detector for decimal numbers based on graphene oxide and DNA-stabilized silver nanoclusters. *Nanoscale* **2017,** *9* (33), 11912-11919.
19. Li, F.; Liu, X. G.; Zhao, B.; Yan, J.; Li, Q.; Aldalbahi, A.; Shi, J. Y.; Song, S. P.; Fan, C. H.; Wang, L. H., Graphene Nanoprobes for Real-Time Monitoring of Isothermal Nucleic Acid Amplification. *ACS Appl. Mater. Interfaces.* **2017,** *9* (18), 15245-15253.
20. Yuan, H. B.; Qi, J. J.; Xing, C. F.; An, H. L.; Niu, R. M.; Zhan, Y.; Fan, Y. B.; Yan, W. M.; Li, R. H.; Wang, B.; Wang, S., Graphene-Oxide-Conjugated Polymer Hybrid Materials for Calmodulin Sensing by Using FRET Strategy. *Adv. Funct. Mater.* **2015,** *25* (28), 4412-4418.
21. Zhu, X. L.; Shen, Y. L.; Cao, J. P.; Yin, L.; Ban, F. F.; Shu, Y. Q.; Li, G. X., Detection of microRNA SNPs with ultrahigh specificity by using reduced graphene oxide-assisted rolling circle amplification. *Chem. Commun.* **2015,** *51* (49), 10002-10005.
22. Lu, C. H.; Yang, H. H.; Zhu, C. L.; Xi, C.; Chen, G. N., A Graphene Platform for Sensing Biomolecules. *Angew. Chem. Int. Ed.* **2009,** *121* (26), 4879-4881.
23. Park, J. S.; Goo, N. I.; Kim, D. E., Mechanism of DNA adsorption and desorption on graphene oxide. *Langmuir.* **2014,** *30* (42), 12587-12595.
24. Zhou, C. Y.; Liu, D. L.; Wu, C. T.; Liu, Y. Q.; Wang, E. K., Integration of DNA and graphene oxide for the construction of various advanced logic circuits. *Nanoscale* **2016,** *8* (40), 17524-17531.
25. Zhou, C. Y.; Wang, K.; Fan, D. Q.; Wu, C. T.; Liu, D. L.; Liu, Y. Q.; Wang, E. K., An enzyme-free and DNA-based Feynman gate for logically reversible operation. *Chem. Commun.* **2015,** *51* (51), 10284-10286.
26. Hao, Z.; Zhu, Y. B.; Wang, X. J.; Rotti, P. G.; DiMarco, C.; Tyler, S. R.; Zhao, X. Z.; Engelhardt, J. F.; Hone, J.; Lin, Q., Real-Time Monitoring of Insulin Using a Graphene Field-Effect Transistor Aptameric Nanosensor. *ACS Appl. Mater. Interfaces.* **2017,** *9* (33), 27504-27511.
27. Kim, J.; Park, S. J.; Min, D. H., Emerging Approaches for Graphene Oxide Biosensor. *Anal. Chem.* **2017,** *89* (1), 232-248.
28. Wei, Y.; Zhang, J.; Wang, X.; Duan, Y. X., Amplified fluorescent aptasensor through catalytic recycling for highly sensitive detection of ochratoxin A. *Biosens. Bioelectron.* **2015,** *65*, 16-22.
29. Connaghan-Jones, K. D.; Moody, A. D.; Bain, D. L., Quantitative DNase footprint titration: a tool for analyzing the energetics of protein-DNA interactions. *Nat Protoc.* **2008,** *3* (5), 900-914.
30. Liu, M.; Hui, C. Y.; Zhang, Q.; Gu, J.; Kannan, B.; Jahanshahi-Anbuhi, S.; Filipe, C. D. M.; Brennan, J. D.; Li, Y. F., Target-Induced and Equipment-Free DNA Amplification with a Simple Paper Device. *Angew. Chem. Int. Ed.* **2016,** *55* (8), 2709-2713.
31. Liu, M.; Zhang, Q.; Chang, D. R.; Gu, J.; Brennan, J. D.; Li, Y. F., A DNAzyme Feedback Amplification

Strategy for Biosensing. *Angew. Chem. Int. Ed.* **2017,** *56* (22), 6142-6146.
32. Dong, H. F.; Zhang, J.; Ju, H. X.; Lu, H. T.; Wang, S. Y.; Jin, S.; Hao, K. H.; Du, H. W.; Zhang, X. J., Highly sensitive multiple microRNA detection based on fluorescence quenching of graphene oxide and isothermal strand-displacement polymerase reaction. *Anal. Chem.* **2012,** *84* (10), 4587-4593.
33. Cui, L.; Chen, Z. R.; Zhu, Z.; Lin, X. Y.; Chen, X.; Yang, C. J., Stabilization of ssRNA on graphene oxide surface: an effective way to design highly robust RNA probes. *Anal. Chem.* **2013,** *85* (4), 2269-2275.
34. Lei, H. Z.; Mi, L. J.; Zhou, X. J.; Chen, J. J.; Hu, J.; Guo, S. W.; Zhang, Y., Adsorption of double-stranded DNA to graphene oxide preventing enzymatic digestion. *Nanoscale* **2011,** *3* (9), 3888-3892.
35. Lu, C. H.; Zhu, C. L.; Li, J.; Liu, J. J.; Chen, X.; Yang, H. H., Using graphene to protect DNA from cleavage during cellular delivery. *Chem. Commun.* **2010,** *46* (18), 3116-3118.
36. Tang, Z. W.; Wu, H.; Cort, J. R.; Buchko, G. W.; Zhang, Y. Y.; Shao, Y. Y.; Aksay, I. A.; Liu, J.; Lin, Y. H., Constraint of DNA on functionalized graphene improves its biostability and specificity. *Small* **2010,** *6* (11), 1205-1209.
37. Tang, L. H.; Chang, H. X.; Liu, Y.; Li, J. H., Duplex DNA/Graphene Oxide Biointerface: From Fundamental Understanding to Specific Enzymatic Effects. *Adv. Funct. Mater.* **2012,** *22* (14), 3083-3088.
38. Seferos, D. S.; Prigodich, A. E.; Giljohann, D. A.; Patel, P. C.; Mirkin, C. A., Polyvalent DNA Nanoparticle Conjugates Stabilize Nucleic Acids. *Nano Lett.* **2009,** *9* (1), 308-311.
39. Tang, L. H.; Wang, Y.; Li, J. H., The graphene/nucleic acid nanobiointerface. *Chem. Soc. Rev.* **2015,** *44* (19), 6954-6980.
40. Liu, H. Y.; Li, L.; Wang, Q.; Duan, L. L.; Tang, B., Graphene fluorescence switch-based cooperative amplification: a sensitive and accurate method to detection microRNA. *Anal. Chem.* **2014,** *86* (11), 5487-5493.
41. Giusto, D. A. D.; Wlassoff, W. A.; Gooding, J. J.; Messerle, B. A.; King, G. C., Proximity extension of circular DNA aptamers with real-time protein detection. *Nucleic Acids Res.* **2005,** *33* (6), e64.
42. Qiu, L. P.; Wu, Z. S.; Shen, G. L.; Yu, R. Q., Highly sensitive and selective bifunctional oligonucleotide probe for homogeneous parallel fluorescence detection of protein and nucleotide sequence. *Anal. Chem.* **2011,** *83* (8), 3050-3057.
43. Yang, L. T.; Fung, C. W.; Cho, E. J.; Ellington, A. D., Real-time rolling circle amplification for protein detection. *Anal. Chem.* **2007,** *79* (9), 3320-3329.
44. Walker, G. T.; Little, M. C.; Nadeau, J. G.; Shank, D. D., Isothermal in vitro amplification of DNA by a restriction enzyme/DNA polymerase system. *Proc. Natl. Acad. Sci. U. S. A.* **1992,** *89* (1), 392-396.
45. Marcano, D. C.; Kosynkin, D. V.; Berlin, J. M.; Sinitskii, A.; Sun, Z. Z.; Slesarev, A.; Alemany, L. B.; Lu, W.; Tour, J. M., Improved Synthesis of Graphene Oxide. *Acs Nano* **2010,** *4* (8), 4806-4814.
46. Gao, W., Synthesis, Structure, and Characterizations. In *Graphene Oxide: Reduction Recipes, Spectroscopy, and Applications*, Gao, W., Ed. Springer International Publishing: Cham, **2015**; pp 1-28.
47. Zhao, J. J.; Liu, L. Z.; Li, F., Structural Characterization. In *Graphene Oxide: Physics and Applications*, Springer Berlin Heidelberg: Berlin, Heidelberg, **2015**; pp 15-29.
48. Wang, Y.; Tang, L. H.; Li, Z. H.; Lin, Y. H.; Li, J. H., In situ simultaneous monitoring of ATP and GTP using a graphene oxide nanosheet-based sensing platform in living cells. *Nat Protoc.* **2014,** *9* (8), 1944-1955.
49. Wang, Z. D.; Lee, J. H.; Lu, Y., Label-Free Colorimetric Detection of Lead Ions with a Nanomolar

Detection Limit and Tunable Dynamic Range by using Gold Nanoparticles and DNAzyme. *Adv. Mater.* **2008,** *20* (17), 3263-3267.

50. Wang, M. D.; Wang, W. H.; Kang, T. S.; Leung, C. H.; Ma, D. L., Development of an Iridium (III) Complex as a G-Quadruplex Probe and Its Application for the G-Quadruplex-Based Luminescent Detection of Picomolar Insulin. *Anal. Chem.* **2016,** *88* (1), 981-987.

51. Wang, Y. J.; Bai, X. N.; Wen, W.; Zhang, X. H.; Wang, S. F., Ultrasensitive Electrochemical Biosensor for HIV Gene Detection Based on Graphene Stabilized Gold Nanoclusters with Exonuclease Amplification. *ACS Appl. Mater. Interfaces.* **2015,** *7* (33), 18872-18879.

For Table of Contents Only